


# Paleoenvironmental changes during the last 3000 years in Lake Cari-Laufquen (Northern Patagonia, Argentina), inferred from ostracod paleoecology, petrophysical, sedimentological and geochemical data

Corina Coviaga,<sup>1</sup> Gabriela Cusminsky,<sup>1</sup> Alejandra Patricia Pérez,<sup>1</sup> Antje Schwalb,<sup>2</sup> Vera Markgraf<sup>3</sup> and Daniel Ariztegui<sup>4</sup>

The Holocene  
2018, Vol. 28(12) 1881–1893  
© The Author(s) 2018  
Article reuse guidelines:  
sagepub.com/journals-permissions  
DOI: 10.1177/0959683618798131  
journals.sagepub.com/home/hol  


## Abstract

South American paleoreconstructions are of global interest because it is the only landmass extending from the tropics to the southern high latitudes and intersecting the entire southern westerly wind belt. In this context, endorheic environments, as Lake Cari-Laufquen Grande (LCLG; 41°35'S, 69°25'W) are excellent sites for paleoenvironmental studies, since they react rapidly to changes in the precipitation/evaporation ratio. In this study, the limnological conditions prevailing during the last 3000 years have been inferred based on a multiproxy analysis of the sedimentary sequence of LCLG (water depth 4 m, core length 505 cm). Today, this is one of the few lakes in Northern Patagonia, providing a unique paleoclimatic and paleoecological lacustrine record. The ostracod assemblages, along with sedimentological, petrophysical and geochemical data, show hydrological changes in Cari-Laufquen Grande basin during the studied period. Our results indicate the continuous presence of a saline to brackish lake. However, changes in ostracod assemblages and sedimentological features reveal variations in the relative salinity of the system. The lake paleosalinity was estimated based on ostracod salinity optima, using a calibration dataset of 29 species and 72 different environments. Intervals of high salinity (24–26 g L<sup>-1</sup>) were dominated by *L. rionegroensis* (morph.I) and organic-poor sediments. Periods of lower salinity (14–20 g L<sup>-1</sup>) favored the occurrence of oligo-mesohaline taxa, such as *R. whatleyi*, *L. rionegroensis* (morph.III), *Cypridopsis* sp., *L. patagonica* and *I. ramirezi*. The sediments further display higher values of both TOC and magnetic susceptibility. These salinity changes are interpreted as water level variations, associated in turn to cold-wet and warm-dry periods in northern Patagonia. Our results provide new insights into the late-Holocene environmental history of the region, characterized by a paucity of records. In addition, the ostracod paleoecology modeled using a WA approach allowed quantitative inferences of salinity changes, highlighting their potential in Quaternary paleoclimate research.

## Keywords

lacustrine sediments, ostracod, sedimentology, paleosalinity, Patagonia, late-Holocene

Received 2 February 2018; revised manuscript accepted 25 June 2018

## Introduction

Endorheic lakes are excellent sites for paleoenvironmental studies (Ariztegui et al., 2008; Cusminsky et al., 2011; Piovano et al., 2002). These environments respond quickly to climatic changes because their hydrology depends almost entirely on the precipitation–evaporation balance. Fluctuations in this ratio are reflected through lake-level changes, which lead to variations in water salinity and solute composition through evaporative concentration or dilution, affecting the biological community of the aquatic environment (Holmes et al., 1998). Both chemical and biological changes are recorded in the sediments and can be decoded using a multiproxy approach (Markgraf et al., 2003; Piovano et al., 2002).

One of these paleoenvironmental proxies are the ostracods preserved in the sediments. These bivalve microcrustaceans are commonly found in almost all types of water bodies and, as a result of the excellent preservation of their calcareous valves, represent one of the most abundant organisms within the fossil record (Horne et al., 2002). The analysis of their species assemblage, abundance, diversity, population structure and valve preservation reveals a variety of limnological data such as salinity, ionic

composition, pH, dissolved oxygen concentration, temperature and wave energy (Boomer et al., 2003; Keatings et al., 2010). Therefore, ostracods are widely used in paleoenvironmental reconstructions especially in Quaternary non-marine environments (e.g. Coviaga et al., 2017; Keatings et al., 2010; Marco-Barba et al., 2013a; Mezquita et al., 2005; Whatley and Cusminsky, 1999).

<sup>1</sup>Instituto de Investigaciones en Biodiversidad y Medioambiente (INIBIOMA-CONICET-UNComahue), Argentina

<sup>2</sup>Institut für Umweltgeologie, Technische Universität Braunschweig, Germany

<sup>3</sup>INSTAAR, University of Colorado Boulder, USA

<sup>4</sup>Department of Earth Sciences, University of Geneva, Switzerland

## Corresponding author:

Corina Coviaga, Instituto de Investigación en Biodiversidad y Medioambiente (INIBIOMA-CONICET-UNComahue), Quintral 1250, San Carlos de Bariloche 8400, Argentina.  
Email: corinacoviaga@gmail.com

In recent years, there has been an increasing interest in the study of these organisms in Patagonia. Several authors have carried out surveys of fossil and extant ostracod fauna in the region providing information about their relationship with the physical and chemical features of their host waters. Schwalb et al. (2002) and Cusminsky et al. (2005, 2011) have identified particular ostracod assemblages in different types of environments, that is, springs, seeps and streams; permanent ponds and lakes; and shallow and ephemeral aquatic environments. Later, Ramón-Mercau et al. (2012), Coviaga (2016) and Coviaga et al. (2015, 2018a) showed that the duration of hydroperiod, conductivity, temperature and dissolved oxygen concentration have a special relevance in the distribution, abundance and life cycle of Patagonian ostracods. These observations have been very helpful in the interpretation of paleoclimatic and paleoenvironmental changes during the Quaternary in Patagonia (Coviaga et al., 2017; Cusminsky et al., 2011; Ohlendorf et al., 2014).

This study focuses on the ostracod fauna, along with the sedimentological, petrophysical and geochemical features, from sediments from Lake Cari-Laufquen Grande (LCLG). This shallow water body is characterized by a negative precipitation/evaporation balance and a fluctuating water level. Previous studies of this lake basin showed changes in lake levels through the late Quaternary. Galloway et al. (1988) identified and dated shorelines at 25–30 m ( $19.1 \pm 0.2$  kyr BP), 15–20 m ( $15.8 \pm 0.2$  kyr BP) and 8 m ( $7.9 \pm 0.6$  kyr BP) above the lake level; indicating periods of deep, saline and alkaline conditions. Likewise, Bradbury et al. (2001) suggested that the highest lake level occurred between 18.4 and 13.0 kyr BP, with a shoreline at +60 m above the lake level, and a second high stand (at +35 m) centered around 10.0 kyr BP. Sedimentological analysis of deposits from these intervals suggested that during these periods, the lacustrine system was turbid and saline, with low productivity (Bradbury et al., 2001). Recently, Cartwright et al. (2011) found evidence of a deep lake from 28 cal. ka to 19 cal. ka BP, with the deepest phase from 27 to 22 cal. ka BP; probably due to colder and wetter conditions during the Last Glacial Maximum (LGM). Studies with ostracods also have identified a deepening of the lake during the late Pleistocene, with a high lake level in the 21–16 cal. ka interval (Pineda, 2008). A subsequent drop in water level suggests a decrease in rainfall and drier conditions in the area during the early Holocene (9.5–6.5 cal. ka BP) (Cusminsky et al., 2011; Whatley and Cusminsky, 1999). Until now, and although many studies were focused on this paleo-lake system, the lake history of the Cari-Laufquen basin since the middle Holocene to Recent times still remains an open question.

South American climate is of particular interest because it is the only land mass extending throughout the main area of the modern Southern Hemisphere Westerlies wind (SWW) belt at 40–55°S and, therefore, plays a crucial role for paleoclimate reconstruction in the Southern Hemisphere (Garreaud et al., 2009). Thus, the paleoclimatic evolution of South America is to a large extent ruled by the behavior (strength and latitudinal position) of the storm tracks of the Southern Westerlies. Particularly during the mid- to late-Holocene, several paleoecological records from southernmost South America revealed an increased climate variability consequence of the Southern Westerlies migration (Gilli et al., 2005). Multiple paleoclimate archives indicate an overall decrease in temperature and intensification in westerly wind intensity that culminates between 400 and 50 yr BP. Likewise, lacustrine records pointed increased variability in moisture balance/lake levels during the last 2000 years (Moy et al., 2009).

The aim of the present contribution is to reconstruct the late-Holocene paleolimnology of LCLG, combining information from ostracod assemblages and sedimentary features. By analyzing changes in these parameters through the sequence, we will show water level variations, corresponding with environmental changes previously registered in the region.

### Geographical, geological and climatic settings

The Cari-Laufquen basin (41°35'S, 69°25'W) is situated in northern Patagonia, Argentina (Figure 1). The basin is located in a tectonic depression, at the eastern margin of the South American convergent plate and to the west of the Somuncura Massif. The stratigraphic sequence starts with Mesozoic rocks, composed mainly of volcanic deposits (Garamilla and Taquetren Formations) of Triassic–Jurassic age and of calcareous sand and silty clay sediments (Angostura Colorada and Coli-Toro Formations) of Cretaceous age, ending with the Pliocene Loma Alta basalt member. The last glaciation did not affect this region (Ariztegui et al., 2008) and, thus, the basin contains a Pleistocene sequence of lacustrine sediments, whereas the Holocene also encompasses alluvial, colluvial and aeolian deposits (Whatley and Cusminsky, 1999).

Currently, the mean annual precipitation in the area is 200 mm/yr, occurring mostly during austral winter months, from May to August. The mean annual temperature is 4°C with prevailing winds from the west (Ariztegui et al., 2008). Nowadays, the Cari-Laufquen system has a catchment of about 16,500 km<sup>2</sup> and is divided into two lakes connected through the Maquinchao River. The Lake Cari-Laufquen Chica (LCLC) is a semi-permanent water body situated at 820 m above sea level, with an area of 5.89 km<sup>2</sup> (Reissig et al., 2006), a pH of 7.8 and a sodium bicarbonate concentration of 283 ppm (Galloway et al., 1988). The LCLG is an ephemeral and brackish water body located at 800 m above sea level. It has an area of 30.75 km<sup>2</sup> (Reissig et al., 2006) and a maximum water depth of 4 m, with a pH of 8.6 and a solute concentration of 4000 ppm (Galloway et al., 1988). More recent studies of the chemistry of the water column report pH values ranging between 9.0 and 9.4 and stable oxygen isotopic values of 9.53‰. Today, the lake contains waters enriched in Cl<sup>-</sup> and Na<sup>+</sup>, with a cationic relationship Na<sup>+</sup> >> Mg<sup>++</sup> > Ca<sup>++</sup> > K<sup>+</sup> and an anionic relationship Cl<sup>-</sup> > SO<sub>4</sub><sup>-</sup> >> HCO<sub>3</sub><sup>-</sup> (Diaz and Pedrozo 1996; Schwalb et al., 2002). More details about the chemical and isotopic compositions of the lake water can be found in Pacton et al. (2015). In recent years, the surface of both lakes has been dramatically reduced due to a prolonged period of abnormally low rainfall beginning in the year 2007 (Departamento Provincial de Aguas, 2011). Analogously, major variations in lake level have characterized different time intervals in the past and, for instance, during the late Pleistocene both lakes were united and consequently much more extended (Whatley and Cusminsky, 1999).

## Methodology

### Core retrieval

An approximately 100 km of high-resolution seismic profiles were collected from LCLG in 1997 using an Ocean Research Equipment (ORE)-GEOPULSE 3.5 kHz single-channel pinger system with a vertical seismic resolution of approximately 10–20 cm (Ariztegui et al., 2001). This geophysical data allowed choosing a coring site encompassing the longest sedimentary record (Figure 1). In 1999, a 505-cm-long sediment core was retrieved (core CLG99-5b) using a short gravity corer and a vibracoring system at ~4 m water depth. The synthetic sedimentary profile of the core is presented in this contribution and was previously published in Ariztegui et al. (2008).

### Chronology

The chronology of the core is based on two AMS radiocarbon dates (<sup>14</sup>C) performed on macrofossils remains (depth: 457 cm) and bulk sediment (depth: 74 cm). Both samples were measured at the ETH-Zürich, Switzerland (Ariztegui et al., 2008). Radiocarbon ages were calibrated against the Southern Hemisphere Calibration curve SHCAL 13 (Hogg et al., 2013) using the

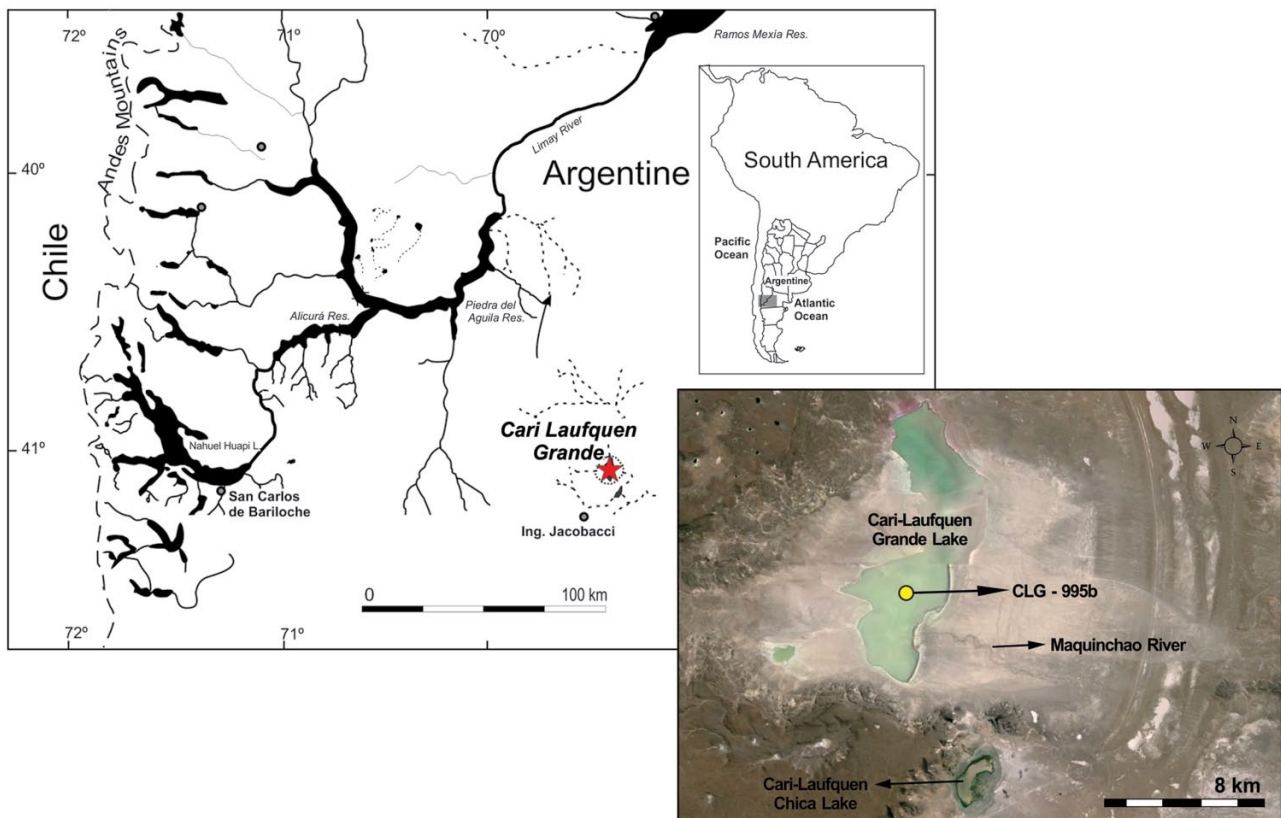


**Figure 1.** Location of LCLG in Río Negro Province, northern Patagonia (Argentina). At right, image of the lake (obtained through Google Earth, free version) showing former shorelines. The yellow circle indicates core location (CLG-995b).

**Table 1.** Radiocarbon ages obtained in both bulk and macrofossil samples.

Sample N°	Sample ID	Depth (cm)	Sample type	$^{14}\text{C}$ yr BP	Cal. age 95.4% confidence interval (cal. BP)	Median probability (cal. BP)	Ratio $^{13}\text{C}/^{12}\text{C}$ (‰)
1	ETH-20898	74	Bulk sediment	$1250 \pm 55$	1270–1194	1257	–20.9
2	ETH-20899	457	Macrofossils	$2770 \pm 55$	2953–2751	2868	–15.1

program OxCal 4.3 (available at <https://c14.arch.ox.ac.uk/oxcal/OxCal.html>) (Table 1). Ages are reported as calendar years before 1950 CE (cal. a BP). The very low organic carbon content of the sediments prevents obtaining additional radiocarbon ages. Furthermore, an attempt to develop a Pb-210 chronology also failed most probably due to the extremely low annual precipitation in the area. Thus, the present chronological model is the best that could be achieved so far.

### Sediment analyses

The core was stored in a dark cold room at 4°C and scanned prior to opening at the ETH-Zürich (Switzerland), using a GEOTEK MST multisensor to measure petrophysical properties (bulk density, magnetic susceptibility and sonic velocity).

Immediately after opening, the core was photographed and described in detail (Ariztegui et al., 2008). Subsequently, it was continuously subsampled at 5 cm interval. Water weight percentage was calculated using standard procedures while total carbon (TC) and carbonate contents were measured using a Coulomat. Total organic carbon (TOC) was calculated by subtracting the carbonate content to the TC percentage.

### Ostracod analyses

Ostracods were analyzed at 5 cm intervals and separated according to a modified version of Forester (1988). About 12 g of wet

sediment was placed in plastic bottles and shaken with 250 mL of 90°C deionized water and one teaspoon of sodium bicarbonate. Samples sat for several hours to promote a full dispersal of the sediments that were subsequently frozen, and subsequently allowed to thaw for several hours. The disaggregated sediment was carefully hand-sieved through a 63  $\mu\text{m}$  mesh, rinsed with deionized water and air-dried.

Ostracod valves, both adult and juvenile stages, were counted and extracted under a stereoscopic microscope. Adult abundance was expressed as number of valves per gram of dry weight of sediment. Data on population structure of the ostracod assemblages were analyzed, including juvenile/adult, male/female and valve/carapace ratios (Boomer et al., 2003). Taxonomic identifications, checked by using a scanning electron microscope (Phillips SEM 515, CNEA Bariloche, Argentina), were based on the literature, including Cusminsky and Whatley (1996), Meisch (2000), Cusminsky et al. (2005), Karanovic (2012) and Coviaga et al. (2018b). Ostracod density was expressed as  $\text{ind g}^{-1}$ , and ostracod species abundance was calculated as percentages.

### Data analyses

The diversity of ostracod assemblages was summarized by the exponential of Shannon index ( $H'$ ; Shannon and Weaver, 1963), and the species distribution per sample by the Evenness ( $E$ ; Margalef, 1974). In addition, the Dubois fluctuation index (D0; Dubois, 1973), formulated as Taylor's expansion of the diversity

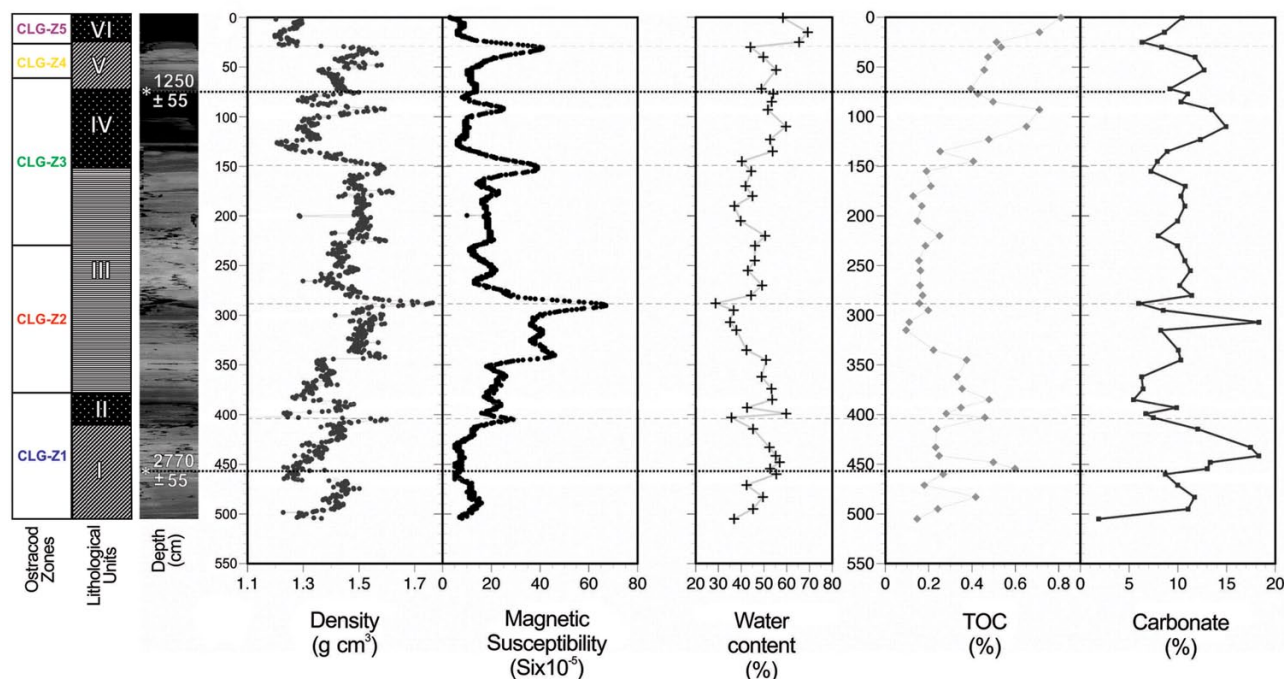


**Figure 2.** Sedimentological, petrophysical and geochemical data for core CLG99-5b. Six lithological units have been identified and are described in the text. Ostracod zones are also included to the left of the figure to facilitate the comparison of the different datasets. Gray lines indicate plausible hiatus and asterisks radiocarbon ages. See text for details.

index  $H'$  around the reference state was applied to define the deviation of the species proportions through time from an average state.

Ostracod species assemblages and abundance were plotted using TILIA 1.7.16 and TILIAGRAPH 2.0.2 software (Grimm, 1991). To distinguish different associations along the sequence, a stratigraphically constrained cluster analysis (CONISS) was further applied to the species assemblage data (Grimm, 1987). Zonation significance levels were evaluated with a one-way analysis of similarities (ANOSIM), using the program PRIMER-E v. 6.12 (Clarke and Gorley, 2005). This analysis tests for differences among factors using permutation and randomization method based on the similarity matrix Bray-Curtis (Clarke and Warwick, 2001). In addition, a detrended correspondence analyses (DCA) was used to measure the gradient length in paleocommunity data. This analysis revealed a gradient length of 1.9 standard deviation, indicating that the dataset has a linear response and suggesting that a principal component analysis (PCA) yields the most valid results for paleoenvironmental interpretations (ter Braak, 1987). Ostracod density was log transformed prior to ordination analysis, due to dataset with several nil entries a  $\log(x + 1)$  transformation is beneficial by lowering the relative importance of the most abundant species in multivariate space (Curry et al., 2016). Multivariate analyses, DCA and PCA, were performed using CANOCO v.5 (ter Braak and Prentice, 1988).

Paleosalinity reconstruction of LCLG from core CLG 99-5b was carried out using an ostracod-based weighted averaging transfer function (C2 software; Juggins, 2003). Most of the species' optima and tolerances used for this reconstruction were estimated based on data from Coviaga et al. (2018a) and Cusminsky (pers. comm.). The final calibration dataset consisted of 29 species and 72 environments, covering a conductivity range from 24 to 68,300  $\mu\text{S cm}^{-1}$ . Reconstructed conductivity ( $\mu\text{S cm}^{-1}$ ) values were transformed to salinity ( $\text{g L}^{-1}$ ) using the following conversion estimated by Marco-Barba et al. (2013b)

$$\text{Salinity (g L}^{-1}\text{)} = \left( 0.000701 \times \text{Conductivity (}\mu\text{S cm}^{-1}\text{)} \right) - 0.060988.$$

The resulting salinity ranges encompass the lake's conductivity at the time of deposition. This procedure is regarded as a tool to roughly estimate past salinity levels since it is ignoring the integration of a certain time period within each sample slice of 1 cm thickness and effects of redeposition (Mischke et al., 2005).

## Results

### Chronology

Radiocarbon ages from core CLG99-5b are summarized in Table 1. The obtained ages maintain a stratigraphic order throughout the core, covering the past ca. 3000 years. Assuming unrealistic constant sedimentation between these AMS  $^{14}\text{C}$  dates, however, would indicate highly variable sedimentation rates ranging from ca. 0.25  $\text{cm yr}^{-1}$  for the interval between 457 and 74 cm and of  $\sim 0.06 \text{ cm yr}^{-1}$  for the remaining uppermost section of the core. Despite the lack of a detailed chronology a more careful analysis of the petrophysical parameters can help to clarify the reasons behind these contrasting changes in sedimentation rates (see below).

### Petrophysical, sedimentological and geochemical data

Based on the macroscopic features of the cores, we have identified six stratigraphical units from bottom to top (Figure 2). Unit 1 (505–410 cm) comprises dark to medium gray massive clays with relatively low magnetic susceptibility and increasing carbonate content toward the top. Unit 2 (410–380 cm) is basically similar to Unit 1 but slightly darker with higher TOC. The base of this unit shows a sharp change in density and a peak in magnetic susceptibility that could be attributed to a first hiatus. Unit 3 (380–150 cm) is composed of grayish brown massive clays, occasionally slightly laminated. Between 300 and 280 cm, there is a sharp increase in density, magnetic susceptibility and water content that might be attributed to a second hiatus. Unit 4 (150–75 cm) is composed of dark gray massive clays with high TOC content. The base of the unit is slightly laminated and also marked by a sharp change in density, magnetic susceptibility and water content that might be attributed to a third hiatus (gray line in Figure 2). Unit 5



(75–30 cm) encompasses medium to light gray massive clays with lower TOC and higher density than the previous unit. The uppermost part of the unit shows a sharp peak in magnetic susceptibility and water content that might be attributed to a fourth hiatus. Finally, Unit 6 (30–0 cm) is a dark gray clay, rich in TOC with low density and magnetic susceptibility along with the high values of water content, TOC and carbonate percentages.

Petrophysical data such as density and magnetic susceptibility show concurrent peaks and low values. The density values remain fairly constant, with a mean of  $1.4 \text{ g cm}^{-3}$ . Extreme values are 1.65, 1.7, and  $1.6 \text{ g cm}^{-3}$ , at 400, 290, and 200 cm, respectively. Magnetic susceptibility increases steadily from the bottom reaching a maximum value ( $67 \text{ SI} \times 10^{-5}$ ) at 290 cm to subsequently decrease to the top, with distinctive peaks at 150 cm ( $38 \text{ SI} \times 10^{-5}$ ) and 30 cm ( $40 \text{ SI} \times 10^{-5}$ ). These distinct changes are coinciding with clear lithological changes varying from light gray to dark and very dark gray clays (Figure 2). Sediments holding relatively lower and higher water content (a minimum of 29% at 290 cm and a maximum of 69% at 15 cm) coincide with lighter and darker color lithological intervals, respectively. Geochemical parameters such as TOC and carbonate content also show distinctive values coinciding with the observed sedimentological changes. While in general TOC is very low, comparatively higher values, as for the carbonates, are characteristic of the darker sediments (0.8% and 18%, respectively); the light gray clays hold relatively lower values in both geochemical parameters (0.1% and 0.9%, respectively) (Figure 2). Despite the different behavior of these parameters, one striking feature that is common to all of them is the often-sharp changes in absolute values pointing toward a fragmented sedimentary record and representing at least four hiatuses tentatively shown by the light-gray lines in Figure 2. The available chronology further indicates unreasonable highly variable sedimentation rates suggesting a fragmented record as well. Thus, the entire petrophysical and chronological data are supporting the hypothesis of alternating periods of prevailing erosional and constructional processes at or near desiccation levels in the lake during the last 3000 years as previously suggested by Ariztegui et al. (2008). Unfortunately, the lack of suitable organic remains has prevented dating them properly.

### Ostracods

A total of 93 sediment samples were analyzed for ostracod abundance and diversity. The material recovered was well preserved, with a small proportion of broken and reworked valves, that is, shells were not opaque, without evidence of dissolution, abrasion or overgrowths (Holmes, 2001; Keatings et al., 2007). The percentage of carapaces in the assemblages was less than 1%. Levels 470, 275, 270, 215, 210, 205, 190, 165 and 125 cm were barren.

Throughout the core, ostracod density varied markedly, with the highest density in the lower levels (11, 13, 8 and  $7 \text{ ind g}^{-1}$  at 455, 355, 300 and 0 cm respectively). Nine species belonging to eight genera were identified: *Limnocythere rionegroensis* (Cusminsky and Whatley, 1996; morphotype I and morphotype III; Ramos et al., 2017), *L. patagonica* (Cusminsky and Whatley, 1996), *Riocypris whatleyi* (Coviaga et al., 2018b), *Cypridopsis* sp., *Amphicypris argentinensis* (Fontana and Ballent, 2005), *Potamocypris unicaudata* (Schäfer, 1943), *Ilyocypris ramirezi* (Cusminsky and Whatley, 1996), *Newnhamia patagonica* (Vávra, 1898) and *Penthesinelula araucana* (Figure 3). According to the species' optima and tolerances estimated in this study, most ostracod taxa presented optima at medium (oligohaline range,  $0.5\text{--}5 \text{ g L}^{-1}$ ) and medium-high (mesohaline range,  $5\text{--}18 \text{ g L}^{-1}$ ) salinities, whereas *N. patagonica* exhibited an optimum at low salinity (limnetic range,  $<0.5 \text{ g L}^{-1}$ ) and *L. rionegroensis* morph.I at high salinity (polyhaline range,  $18\text{--}30 \text{ g L}^{-1}$ ). *Newnhamia patagonica*, *L. patagonica* and *L. rionegroensis* (morph.I and III) presented

narrowest tolerance ranges, while *I. ramirezi*, *P. unicaudata*, *Cypridopsis* sp. and *R. whatleyi* displayed the widest tolerance ranges (Figure 4).

Diversity indices are generally low, with an average of  $2 \pm 1.2$  species per level, 29 monospecific (100% *L. rionegroensis* morph.I) samples and a maximum richness of seven species at 300 cm and 295 cm. The mean value of Shannon diversity ( $H'$ ) index was  $0.47 \pm 0.46$ ; the highest diversity was recorded at 285 cm ( $H' = 1.65$ ), while the 29 monospecific samples presented a minimum value ( $H' = 0$ ). The evenness also presented its maximum value at 285 cm ( $E = 1$ ).  $D_0$  index presented values close to zero between 505 and 410 cm, and between 125 and 70 cm, indicating periods closest to the average community (dominated by *L. rionegroensis*). In opposition the higher  $D_0$  values, indicating large differences in ostracod assemblages with respect to the average state, were recorded at 390, 265–260, 245, 45–35 and 20 cm (Figure 5).

*Limnocythere rionegroensis* morph.I was the ubiquitous and most abundant species, reaching 40% to 100% in the assemblages, followed by *R. whatleyi* (up to 60%), *I. ramirezi* and *Cypridopsis* sp. (up to 33% each). The remaining species were much less frequent with four occurrence of *Penthesinelula araucana*, three of *L. patagonica* and *Potamocypris unicaudata*, two of *Newnhamia patagonica* and one occurrence of *Amphicypris argentinensis*. Because *Limnocythere rionegroensis sensu lato* was the most abundant species of the core, a detailed analysis of their population structure could be completed. The juvenile/adults ratio of this species varied through the core from 10 to 0, with a mean of 4.15, and was positively correlated with ostracod density ( $DF = 1$ ,  $F = 60.525$ ,  $p < 0.001$  y  $R^2 = 0.42$ ). Generally, male/female ratio was less than one through all the sequence; except at 310, 115, 45 and 15 cm where this relation was reversed and two males for every female were recorded. In addition, a slight increase in male proportions from 125 cm upward was observed.

### Ostracod assemblages

Application of stratigraphically constrained cluster analysis (Figure 5) allowed the differentiation of five stratigraphical zones (Figure 2). The first zone, CLG-Z1 (505–370 cm), was characterized by low ostracod abundance at the bottom and the top of the zone (around  $0.5 \pm 0.5 \text{ ind g}^{-1}$  and  $1.5 \pm 1.7 \text{ ind g}^{-1}$ , respectively), and a high density in the middle part ( $6.5 \pm 2.5 \text{ ind g}^{-1}$ ). *Limnocythere rionegroensis* morph.I dominated the assemblage through all zone. *Cypridopsis* sp. was recorded in almost all levels and *R. whatleyi* was documented in several of them. On the other hand, *L. patagonica* and *A. argentinensis* were present in the central region of OZ1; and *P. araucana* and *I. ramirezi* in the upper centimeters. An elevate salinity was inferred for this zone, of about  $24.3 \pm 1.9 \text{ g L}^{-1}$ ; with a marked decrease at the upper levels ( $23.0 \pm 1.7 \text{ g L}^{-1}$ ).

Zone CLG-Z2 (370–225 cm) showed strong variations in ostracod density, with high values in levels 355 cm ( $12.9 \text{ ind g}^{-1}$ ) and 300 cm ( $8.4 \text{ ind g}^{-1}$ ), and a very low density in the remaining levels ( $1.0 \pm 1.1 \text{ ind g}^{-1}$ ). In addition, this zone displays a high diversity, including the maximum value for this index along the core (seven species at 300 cm). *Limnocythere rionegroensis* morph.I continued being the most abundant species, although *R. whatleyi* and *L. rionegroensis* morph.III abundances increased. Between 300 and 290 cm depth, coupled with the second peak of density, an increase in ostracod diversity was recorded. In this interval *Cypridopsis* sp., *P. araucana*, *I. ramirezi*, *P. unicaudata*, *R. whatleyi*, *L. rionegroensis* morph.II, together with the dominant *L. rionegroensis* morph.I, represented the assemblage. The salinity inferred for CLG-Z2 was variable ( $22.9 \pm 2.1 \text{ g L}^{-1}$ ), with a minimum of 18.5 (290 cm) and a maximum of  $25.7 \text{ g L}^{-1}$  (at 345, 280–255 cm).

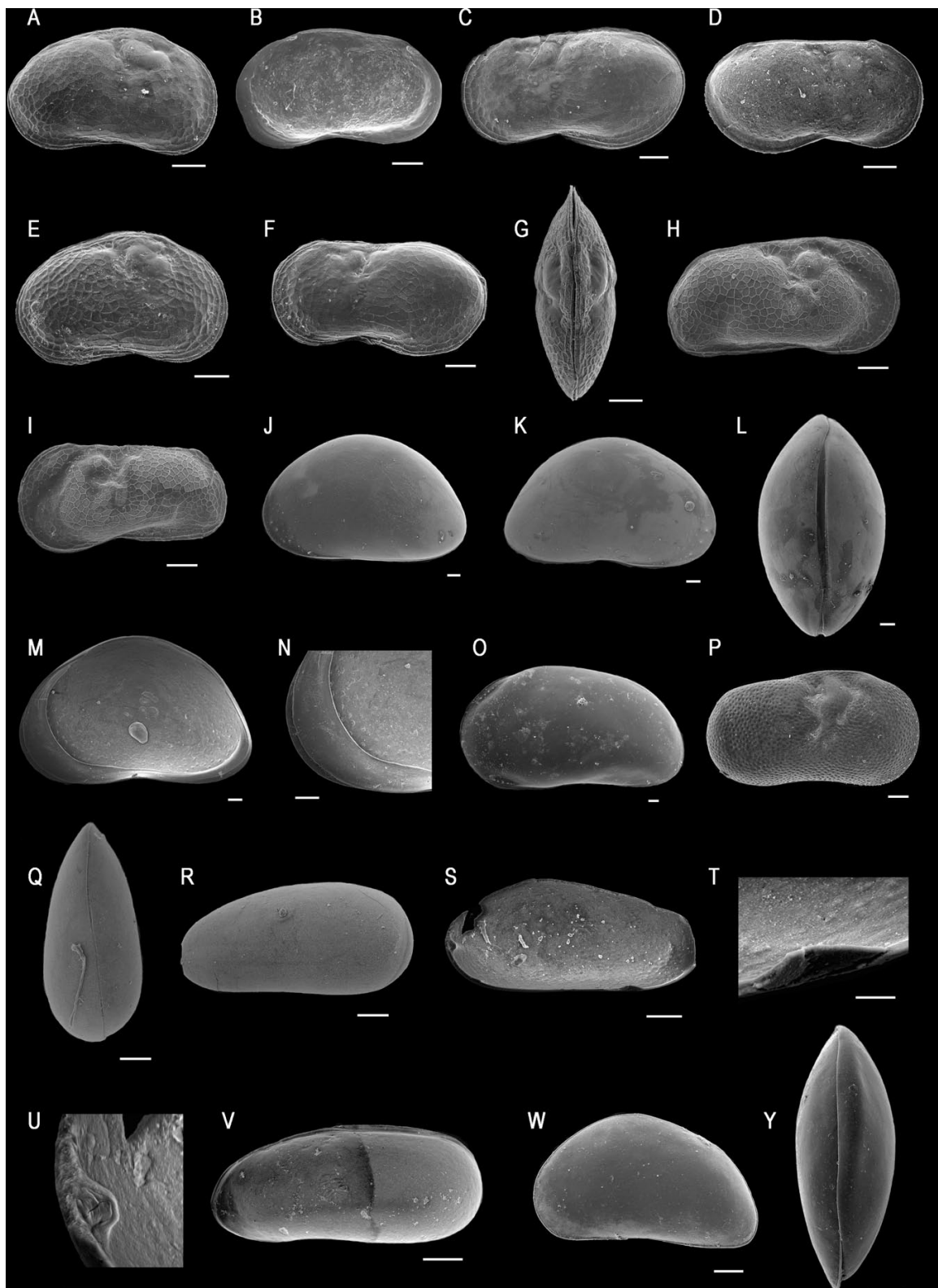


**Figure 3.** Ostracod species identified; scale bar 100  $\mu\text{m}$ , T and U scale bar 20  $\mu\text{m}$ . RV: right valve, LV: left valve, C: carapace. **A-D** *Limnocythere rionegroensis* (morph.I). **A** adult female, RV in external view. **B** adult female, RV in internal view. **C** adult male, LV in external view. **D** adult male, LV in internal view. **E-G** *Limnocythere rionegroensis* (morph.III). **E** adult female, RV in external view. **F** adult male, LV in external view. **G** adult female, C in dorsal view. **H-I** *L. patagonica*. **H** adult female, RV in external view. **I** adult female, LV in external view. **J-M** *Riocypris whatleyi*. **J** adult, LV in external view. **K** adult, RV in external view. **L** adult, C in dorsal view. **M** adult, RV in internal view. **N** adult, RV in internal view, detail of anterior zone. **O** *Amphicypris argentinensis* juvenile, LV in external view. **P** *Ilyocypris ramirezi* adult, RV in external view. **Q-V** *Penthesinelula araucana*. **Q** adult, C in dorsal view. **R** adult, LV in external view. **S** adult, LV in internal view. **T** adult, LV in internal view, detail of antero-ventral teeth. **U** adult, LV in internal view, detail of posterior teeth. **V** adult, RV in internal view. **W-Y** *Potamocypris unicaudata*. **W** adult, LV in external view. **Y** adult, C in dorsal view.

Zone CLG-Z3 covers from 225 to 65 cm depth. This zone includes most of the barren levels along the core (215, 210, 205, 190 and 165 cm). The lowermost part (225–150 cm), presented the lowest ostracod abundances ( $0.1 \pm 0.1$  ind  $\text{g}^{-1}$ ), with an

assemblage composed only of *L. rionegroensis* morph.I. Accordingly, the salinity inferred for this interval was high and constant ( $25.7 \text{ g L}^{-1}$ ). At the top of this zone (150–65 cm), the ostracod abundance remained low although the biodiversity increased. In

this section, *L. rionegroensis* morph.I continued being the most abundant species, including few appearances of *L. rionegroensis* morph.III, *L. patagonica*, *R. whatleyi*, *Cypridopsis* sp., *I. ramirezi*, *N. patagonica* and *P. unicaudata*. The presence of these species is reflected in slight variations of the inferred salinity:  $25.2 \pm 0.8$  g L<sup>-1</sup>.

Zone CLG-Z4 (65–30 cm) was characterized by a remarkably low ostracod density, with values lower than 1.1 ind g<sup>-1</sup>, but high diversity values. *Riocypris whatleyi*, *Cypridopsis* sp. and *P. araucana* showed an abundance increase, with a peak of abundance in the upper levels (around 60% and 33% of ostracod assemblages, respectively). In parallel, *L. rionegroensis* morph.I density drastically decreased. Lower salinity was inferred for this zone of  $19.6 \pm 3.0$  g L<sup>-1</sup>, including the lowest value for this parameter along the core of  $13.9$  g L<sup>-1</sup> at 35 cm.

Zone CLG-Z5 (30–0 cm) exhibited a rise in ostracod occurrence from the bottom to the top, and a low diversity, represented by only two species, *L. rionegroensis* morph.I and *I. ramirezi*. In this zone, *L. rionegroensis* morph.I showed an increase in its abundance of up to 80% of ostracod assemblages. The salinity inferred for CLG-Z5 was higher than in the previous zone ( $24.5 \pm 2.0$  g L<sup>-1</sup>).

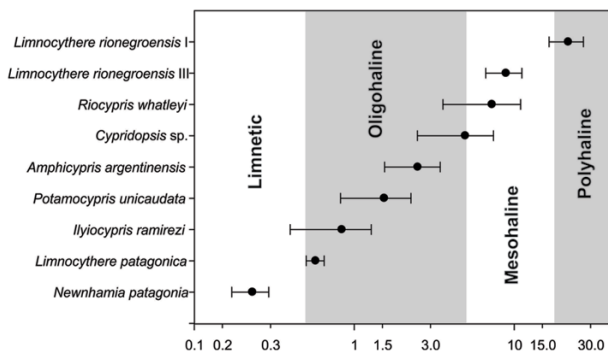


**Figure 4.** Salinity optima and tolerance, estimated through weighted average, of most of the ostracod species recorded in the LCLG sequence. Modified from Coviaga et al. (2018a).

In the PCA results (Figure 6), the first two axes explained 66% of the total variance observed in the ostracod species assemblages; axis 1 accounted for 44% of the total variability and axis 2 for 22%. The species with higher axis 1-weight were *L. rionegroensis* (morph.III), *R. whatleyi* and *P. unicaudata* (positive) and *L. rionegroensis* (morph.I) (negative). Whereas *Cypridopsis* sp., *P. araucana* (positively) and *I. ramirezi* (negatively) were correlated to the second axis. In addition, *L. rionegroensis* (morph.I) and *R. whatleyi* were negatively correlated to each other ( $r = 0.79$ ,  $p < 0.001$ ), providing evidence that they are indicators of contrasting environmental conditions. Likewise, the samples were grouped on the PCA graph similar to the zones obtained with the constrained cluster analysis, although some overlapping were observed. CLG-Z1 and CLG-Z3 samples were mostly located in the lower left quadrant, characterized by an absolute dominance of the brackish *L. rionegroensis* (morph.I). In the same quadrant, CLG-Z5 levels were positioned, composed by *L. rionegroensis* (morph.I) and a high contribution of *I. ramirezi*. In the lower right quadrant, most of CLG-Z2 samples were situated, with high abundances of *R. whatleyi*. CLG-Z4 levels were placed in the right quadrants, showing high *R. whatleyi* and *Cypridopsis* sp. densities.

## Discussion

### Paleolimnological reconstruction

Ostracod fauna recovered from the LCLG sedimentary core consisted of nine species, most of them previously recorded in Upper Pleistocene – Holocene sediments from the Cari-Laufquen basin (Cusminsky et al., 2011; Cusminsky and Whatley, 1996; Pineda, 2008; Whatley and Cusminsky, 1999). Likewise, many of these taxa were recorded both in recent environments (Coviaga et al., 2018a; Cusminsky et al., 2005; Ramón-Mercau et al., 2012) and in Holocene sediments (Coviaga et al., 2017; Cusminsky et al., 2011; Cusminsky and Whatley, 1996; Laprida et al., 2014; Markgraf et al., 2003; Ohlendorf et al., 2014) from Patagonia. The faunal assemblages from the LCLG sequence exhibited diversity indices generally low, with assemblages species-poor dominated by *L. rionegroensis*. Most levels contain one or two species and only two of them reached a maximum diversity of seven taxa. The development of species-rich ostracod assemblages tends to occur only in

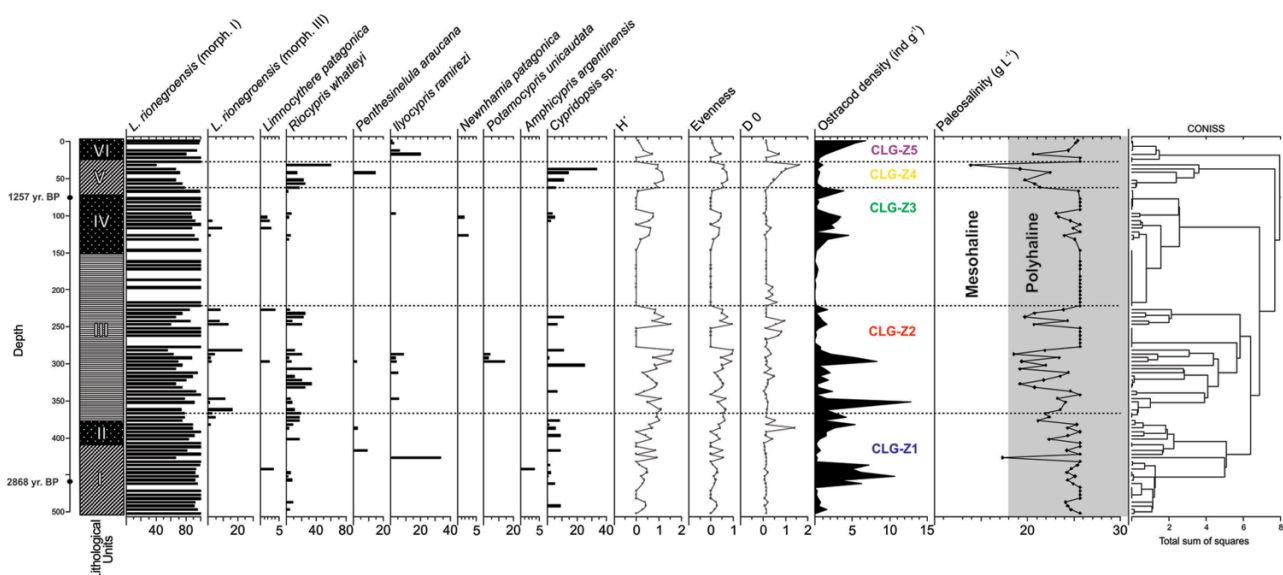


**Figure 5.** Ostracod abundance and diversity indices in the LCLG sequence. Shannon diversity, Evenness and Dubois fluctuation index (D0) are shown. Total numbers of ostracods per gram of dry sediment are shown as filled curve. Reconstructed paleosalinity is presented. Zones calculated by a CONISS cluster analysis are indicated at right. Color codes indicate the CONISS zone: CLG-Z1 in blue; CLG-Z2 in red; CLG-Z3 in green; CLG-Z4 in yellow; CLG-Z5 in violet.

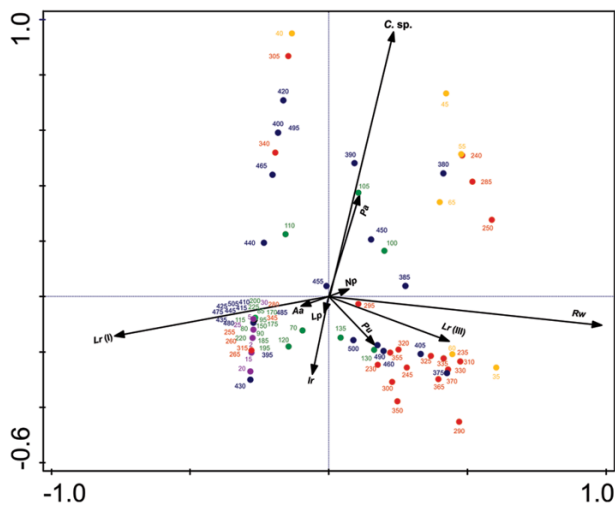


**Figure 6.** Principal component analysis (PCA) biplot of ostracod species (black arrow) and samples (circles) from LCLG sedimentary core. Taxa keys as follows: *Lr(I)* = *Limnocythere rionegroensis* (morph.I); *Lr(III)* = *L. rionegroensis* (morph.III); *Lp* = *L. patagonica*; *Rw* = *Riocypris whatleyi*; *C. sp.* = *Cypridospis sp.*, *Pa* = *Penthesinelula araucana*; *Np* = *Newnhamia patagonica*; *Pu* = *Potamocypris unicaudata*; *Ir* = *Ilyocypris ramirezi*; *Aa* = *Amphicypris argentinensis*. Circle color codes indicate the CONISS zone: CLG-Z1 in blue; CLG-Z2 in red; CLG-Z3 in green; CLG-Z4 in yellow; CLG-Z5 in violet.

stable, extensive habitats; hence, the low diversity of LCLG sequence probably reflects the lack of long-term stability (Holmes et al., 1998). Moreover, the strong dominance of the polyhaline *L. rionegroensis* along the entire core suggests the presence of a lake with saline waters through the last 3000 years (Whatley and Cusminsky, 1999). This species inhabits high evaporative environments, such as temporary lakes and ponds (Ramón-Mercau et al., 2012; Schwalb et al., 2002) and has been postulated as a possible indicator of saline waters and dry climatic conditions (Coviaga et al., 2017; Cusminsky et al., 2005; Ohlendorf et al., 2014; Ramón-Mercau and Laprida, 2016; Whatley and Cusminsky, 1999). Furthermore, the variety of species present also gives information about limnological conditions; the morphotype I of *L. rionegroensis* representing higher ionic concentrations than morphotype III (Ramos et al., 2017). Morphometric analysis of both morphotype valves indicates that morph.I and morph.III present variations in shape, size and ornamentation confirming this hypothesis (Ramos et al., 2017). The low TOC concentration recorded throughout the sequence indicates a relatively poor primary productivity, according to the existence of a shallow and saline lake during the late-Holocene. Analogously, the high TOC observed could be associated to elevated water salinity (Guerra et al., 2015).

A range of environmental factors that include habitat and water composition controls ostracod assemblage, abundance and diversity. These parameters, also affect population structure (valve/carapace and juvenile/adult ratios) and degree of shell preservation. In addition, the latter feature gave an indication of wave energy at the site of deposition (Boomer et al., 2003; De Deckker, 2002; Keatings et al., 2010). In this context, Lake Cari-Laufquen population structure shows a continuous presence of adults and juveniles, both of earlier and later stages, indicating conditions of low-energy thanatocoenosis (Boomer et al., 2003). These autochthonous ostracod assemblages with minimal post-mortem disturbance constitute a good indicator of environmental conditions in which they developed. The juvenile/adult ratio of *L. rionegroensis sensu lato* varied along the sequence and was positively related to ostracod density, pointing that favorable periods for ostracod development were also advantageous for the conservation of juvenile valves. Levels with low juvenile/adult ratios

may be a result of poor preservation or some winnowing of the smaller instars. This suggests high-energy conditions, as a consequence of low lake levels during these periods (Keatings et al., 2010).

The paleolimnological interpretation of the ostracod zones, supported by petrophysical, sedimentological and geochemical data (Figure 2), allowed identifying salinity variations, and the reconstruction of past limnological scenarios, ranging from shallow lake conditions during dry phases and high lake levels during humid periods. From the bottom to the top five zones were distinguished: CLG-Z1 – transition from a shallow to medium deep lake; CLG-Z2 – high lake levels and moderate salinity; CLG-Z3 – very shallow and saline lake, with a short pulse of less saline waters; CLG-Z4 – lake level rise and moderate salinity conditions; CLG-Z5 – transition from high to low water level.

The studied record begins (~ 3000 yr BP) with low ostracod abundance and an assemblage dominated by *L. rionegroensis* morph.I, allowing infer high salinity conditions ( $24.3 \pm 1.9 \text{ g L}^{-1}$ ) for the zone CLG-Z1. In agreement, this section presented low diversity indices values, fluctuating close to zero for index D0, and therefore indicating a period dominated by the polyhaline *L. rionegroensis*. In this zone, organic-poor sediments were observed. Low values of TOC could be associated to periods of comparatively higher contribution of clastics, as a consequence of a low lake level and a dryer environment (Irurzun et al., 2014). These results indicate a positive evaporation/precipitation balance, which could be related to prevailing dry and warm conditions. The uppermost half of the CLG-Z1 zone displayed ostracod assemblages indicative of a lower salinity environment. Particularly, the presence of the oligohaline *L. patagonica* and *A. argentinensis* indicates a lake with low ionic concentrations with surrounding vegetation in the catchment (Coviaga et al., 2018a; Schwalb et al., 2002). *Limnocythere patagonica* is a Patagonian stenohaline taxa, characteristic of permanent ponds and lakes of moderate salinity (Coviaga et al., 2018a; Cusminsky et al., 2005; Ramón-Mercau and Laprida, 2016; Ramón Mercau et al., 2012; Schwalb et al., 2002). An elevated abundance of this species in Lake Cháitel, southeastern Patagonia, has been interpreted to reflect periods of low salinity (Ohlendorf et al., 2014). *Amphicypris argentinensis* was recorded living under moderate conductivity conditions ( $2.0\text{--}8.9 \text{ mS cm}^{-1}$ ) and temperate waters ( $\sim 20^\circ\text{C}$ ) (Coviaga et al., 2018a; Fontana and Ballent, 2005). The comparatively higher percentages of TOC recorded in this zone also indicate an increase in lake primary productivity, and an associated increment in aquatic vegetation (Jenny et al., 2002; Li and Liu, 2014; Meyers and Lallier-Vergès, 1999; Ohlendorf et al., 2014; Zhu et al., 2013). At 430 cm, the high occurrence of *I. ramirezi* suggests an increase in flowing water into the lake, which could be related to a humid phase, and therefore more rainfall in the area. This taxon presents one of the widest ranges in salinity tolerance, supporting its ability to develop within a broad spectrum of limnological conditions (Coviaga et al., 2018a; Cusminsky et al., 2005; D'Ambrosio et al., 2015; Ramón-Mercau et al., 2012; Schwalb et al., 2002). *Ilyocypris ramirezi* is widespread in Patagonia, but exhibits a notably preference for lotic environments, being almost exclusively found in flowing waters (Coviaga et al., 2018a; Cusminsky et al., 2005; Schwalb et al., 2002). Analogously, the increase in sedimentary density and magnetic susceptibility in the upper levels of CLG-Z1 could be a consequence of runoff intensification, resulting from higher precipitation (Iglesias et al., 2011; Sepúlveda et al., 2009). At the top of this zone (CLG-Z1), the significant presence of *R. whatleyi*, indicates a persistence of moderate saline conditions in the lake. This species exhibited a mesohaline salinity optimum, with a wide tolerance range (from oligohaline to mesohaline conditions). In agreement, *R. whatleyi* is considered an euryhaline species, capable of living in waters with a wide range of ionic concentrations (Coviaga



et al., 2018a; Cusminsky et al., 2005). Nevertheless, this taxon prefers moderate-salinity conditions (optima estimated: 8.7 mS cm<sup>-1</sup>; Coviaga et al., 2017).

Highly fluctuating hydrological behavior has been inferred for the second zone, CLG-Z2. Diversity index values increased at levels containing more oligohaline species suggesting environmental fluctuations most probably due to increased hydrological instability. The sharp decrease in *L. rionegroensis* morph.I abundance, coupled with a rise in *R. whatleyi* density and the presence of the *L. rionegroensis* morph.III, *Cypridopsis* sp., *I. ramirezi* and *P. unicaudata* suggests a decline in lake salinity, as indicated by the lower values of the reconstructed salinity. This zone showed a relatively low TOC concentration, which might be associated to a decline in lake productivity as a consequence of low air and water temperatures (Peng et al., 2013; Zhu et al., 2013). The presence of *I. ramirezi*, that is characteristic of flowing waters, by the middle of this zone suggests that at the time the lake was most probably fed by springs and streams (Markgraf et al., 2003; Schwab et al., 2002). Furthermore, the organic-poor sediments observed in the same section can be related to a greater percentage of clastic influx during discharges into the lake owing to flood events (Irruzun et al., 2014). Analogously, the increment in magnetic susceptibility observed in this interval could be linked to an increase in terrestrial contribution, consequence of a rise in runoff derived from increasing rainfall (Iglesias et al., 2011; Sepúlveda et al., 2009). The contemporaneous increase in magnetic increases can be also ascribed to increasing evaporation leading to desiccation (Ariztegui et al., 2008). However, the presence of ostracod assemblages characteristic of less saline conditions and the low TOC content point toward increasing runoff that could also carry clastic sediments from the catchment with higher magnetic susceptibility.

The almost absence of ostracod in the first part of CLG-Z3 suggests an unfavorable period for ostracods development. Diversity index values in this zone were low, due to the increased dominance of *L. rionegroensis* morph.I, as a result of changing conditions that favored the presence of this polyhaline species. The isolated occurrence of *L. rionegroensis* morph.I indicates a shallow lake of high salinity (salinity inferred 25.2 ± 0.8 g L<sup>-1</sup>), suggesting drier conditions in the region (Cusminsky et al., 2005; Whatley and Cusminsky, 1999). In Lake Chátel, monospecific assemblages of this species reflected extreme environmental conditions and a lake hydrochemistry driven by evaporative conditions (Ohlendorf et al., 2014). CLG-Z3 lowermost levels present low TOC content pointing toward a period with low primary productivity and/or poor preservation, that is compatible with a very shallow-ephemeral saline lake (Guerra et al., 2015) with increasing water salinity (Chávez-Lara et al., 2012). The rise in ostracod abundance and diversity between 135 and 100 cm suggests better conditions for the developed of these organisms. Particularly, the occurrence of an ostracod fauna oligohaline or mesohaline, that is, *L. rionegroensis* morph.III, *L. patagonica*, *R. whatleyi*, *I. ramirezi* and *N. patagonica*, indicates pulses of lower salinity. Similarly, the increment in TOC suggest higher primary productivity (Mischke et al., 2008). Periods of wetter climate generally result in enhanced algal productivity, as a consequence of greater influx of soil nutrients (Meyers and Lallier-Vergès, 1999). In the uppermost levels of CLG-Z3, *L. rionegroensis* morph.I becomes again almost the only species recorded, probably as a result of a new increase in lake salinity. A decline in primary productivity driven by the rising salinity also was inferred from the decrease in TOC.

The following zone (CLG-Z4) evidences a low ostracod density, with a notably rise in *R. whatleyi* and *Cypridopsis* sp. abundances and a decrease in the number of *L. rionegroensis* morph.I. This indicates a decline in water salinity, possibly consequence of an increase in lake level, and therefore a reduction in the evaporation/precipitation balance. Higher values of magnetic susceptibility

indicate a significant supply of sediments to the basin, probably consequence of a rise in runoff derived from more precipitation (Sepúlveda et al., 2009; Vargas-Ramirez et al., 2008). CLG-Z4 presents average TOC values, suggesting a moderate primary productivity, probably due to lower air and water temperatures (Peng et al., 2013; Zhu et al., 2013).

The youngest zone (CLG-Z5) displays an assemblage with only two species *L. rionegroensis* morph.I and *I. ramirezi*. The elevated occurrence of *I. ramirezi* in the first levels of the zone suggests a rise in the number and/or intensity of the flowing water conditions into the lake (Schwab et al., 2002). There is a remarkable increase in density of *L. rionegroensis* morph.I toward the top of the core. This would indicate a return to shallower and more saline conditions, probably as a consequence of a decline in rainfall. Likewise, the comparatively higher TOC are recorded, interpreted as enhanced lacustrine primary productivity and might be associated with warmer temperatures (Peng et al., 2013; Recasens et al., 2011).

### Regional and global significance

LCLG has experienced major changes in its development throughout the late Quaternary (Bradbury et al., 2001; Cartwright et al., 2011; Cusminsky et al., 2011; Galloway et al., 1988; Pineda, 2008; Whatley and Cusminsky, 1999). Paleoshorelines have been observed and mapped at elevations up to 100 m above the present lake level (Bradbury et al., 2001; Cartwright et al., 2011; Coira, 1979; Galloway et al., 1988), indicating higher lake levels than nowadays during the late Pleistocene. In agreement, studies with ostracods also have identified a deepening period of the lake during the late Pleistocene, with a high lake level in the 21–16 kyr BP interval (Pineda, 2008). Throughout these lake-level high-stands, Cari-Laufquen Grande Lake was united to LCLC, forming a larger paleolake named Maquinchao (Ariztegui et al., 2008). Today, they are two separate basins but connected through the Río Maquinchao (Figure 1). Toward the early-middle Holocene (9.5–6.5 kyr BP), ostracod and pollen analysis suggests a regressive phase in Cari-Laufquen Lake, brought about by a diminution in the amount of precipitation and enhanced evaporation (Cusminsky et al., 2011; Whatley and Cusminsky, 1999). These dried conditions were probably a consequence of a decrease in the influence of the westerly winds caused by the motion to the poleward position of the subtropical high-pressure cell and the circumpolar vortex being displaced toward Australia (Markgraf, 1983).

The lake history of Cari-Laufquen from the middle Holocene to Recent times remains an open question. Cartwright et al. (2011) found a hiatus in the lacustrine deposition from 18 ka year BP until the last 500 years, suggesting that there is no evidence that a deep lake developed during this long hiatus such as those present > 19 ka. However, the very shallow record studied was not well exposed, being possible that this characterization was incomplete (Cartwright et al., 2011).

In this study, the paleolimnological interpretation of the ostracod assemblages in concert with petrophysical, sedimentological and geochemical data allowed us to identify lake level changes during the last 3000 years. Thus, these results contribute to elucidate the lake history in terms of salinity fluctuations from the middle Holocene to Recent times. Because LCLG is a closed basin, such changes are related to variations in the precipitation/evaporation ratio and the regional hydrological balance, which in turn, reflects the prevailing climate. Consequently, LCLG water level variations might be associated to cold-wet and warm-dry periods previously proposed in the region using other proxies. The comparison among our proxy data and other records from sites located in Patagonia allow us to infer some regional paleoclimate changes during the late Holocene, in spite of possible uncertainties due to the radio- carbon dating.

In Patagonia, an arid phase, drier and warmer, was identified during 3.6–3.0 cal. ka BP at both sides of the Andes, in Cerro Verlika (~ 50°S), Argentina (Mancini, 2001) and in Hielos Patagónicos Sur (~ 48 - 51°S), Chile (Glasser et al., 2004). A comparable positive evaporation/precipitation balance was inferred in Cari-Laufquen Grande at the beginning of the studied record (~ 3.0 cal. ka BP). Subsequently, between 2.7 and 2.2 cal. ka BP, a wet and cold climate is proposed as the responsible of the glacier advances recorded in Hielos Patagónicos Sur (Mercer, 1970). This could be represented at the uppermost half of the CLG-Z1 zone, where our multiproxy analysis suggests a decrease in salinity conditions, related to a humid phase that trigger a rainfall increase in the area. Between 1.75 and 1.55 cal. ka BP, a wet period was recorded in Laguna Aculeo (~ 34°S Chile), (Jenny et al., 2002). These authors identified a high frequency of clastic layers during this interval, reflecting flooding events and therefore, more humid conditions in the region (Jenny et al., 2002). Our data suggest a greatly fluctuating hydrological behavior, with high lake levels and moderate salinity, toward the second zone (CLG-Z2). In addition, an increasing terrestrial contribution as a consequence of rising runoff derived from increasing rainfall was inferred, indicating a significant contribution of tributary waters into LCLG. During 1.35 cal. ka BP and 800 years BP a period of warmer temperatures was identified in Lago Castor (45°36'S, 71°47'W) and Laguna Escondida (45°31'S, 71°49'W), Chile. The climate reconstruction, based in sedimentological proxies, carried out in these lakes, showed a pronounced (multi)decadal-scale variability and warm periods between 1.4 cal. ka BP and 750 years BP, except between 1.1 and 1.05 cal. ka BP where a cold period was inferred (Elbert et al., 2013). These inferences can be compared with our evidences of a shallow and saline lake, with pulses of lower salinity, suggesting drier conditions in the region (CLG-Z3). Several studies carried out in the region have shown a sustained cooling, coupled with a transition from drier to wetter conditions between 1.07 cal. ka BP and 675 years BP (Elbert et al., 2013; Guerra et al., 2015; Sepúlveda et al., 2009; Villalba, 1994). This humid pulse was contemporaneous with the Medieval Climatic Anomaly (MCA) that has been dated in southern South America from ~ 850 to 600 years BP (Villalba, 1994). This negative evaporation/precipitation balance is compatible with our results (CLG-Z4) showing a decline in water salinity, due to low temperatures and more precipitation in the area. Jenny et al. (2002) has recorded a great frequency of flood events in Laguna Aculeo (Chile) from 650 to 250 years BP and linked it to more humid conditions due to an increase in the intensity of the Westerlies. Bertrand et al. (2005) and Sepúlveda et al. (2009) also have found evidence of cold conditions coupled with high rainfall between 450 and 250 years BP, suggesting a regional expression of the Little Ice Age (LIA) in northern Patagonia. According with these regional climate conditions, in the first levels of the youngest zone (CLG-Z5), a rise in the number and/or intensity of the flowing water conditions into the lake was suggested. Tree-rings studies have shown a dryer climate in the region between 150 and 50 years BP (Lara and Villalba, 1993; Luckman and Villalba, 2001; Villalba, 1994). This is supported by lacustrine sediments records, which indicates a drier period during 250–50 years BP (Ariztegui et al., 2007; Boës and Fagel, 2007; Bertrand et al., 2005; Charlet et al., 2008; Guilizzoni et al., 2009). Corresponding with these evidences, toward the top of the LCLG core, the multiproxy analysis indicates a return to a shallower and more saline lake, probably as a consequence of a decline in rainfall along with warmer temperatures in Cari-Laufquen area.

## Conclusion

The ostracod record, coupled with the sedimentological, petro-physical and geochemical features, allowed the paleolimnological reconstruction of LCLG covering the last 3000 years. The existing knowledge of the ecology of extant representatives of the ostracod species recovered in the LCLG sequence, the observed changes in ostracod assemblages during the studied period allowed us to reconstruct the variations in lake salinity. Intervals of high salinity were markedly dominated by *L. rionegroensis* morph.I, whereas periods of less saline conditions favored the occurrence of oligo-mesohaline taxa, such as *R. whatleyi*, *L. rionegroensis* morph.III and *I. ramirezi*. In this context, the inferred paleosalinity allowed the reconstruction of past limnological scenarios, ranging from shallow lake conditions during dry phases and comparatively higher lake levels during humid periods. Five zones were distinguished from bottom to top as follows: CLG-Z1 – transition from a shallow to medium deep lake; CLG-Z2 – high lake levels and moderate salinity; CLG-Z3 – very shallow and saline lake, with a short pulse of less saline waters; CLG-Z4 – lake level rise and moderate salinity conditions; CLG-Z5 – transition from high to low water level.

The results obtained in this study show the usefulness of lacustrine ostracods and sedimentary parameters as proxies for changing hydrological conditions. It also shows, however, the need to increase the existing knowledge of modern ostracod ecology and biology (Holmes et al., 1998). A more complete data-base would allow us to do a more detailed interpretation of fossil assemblages in terms of salinity, ionic composition and other habitat variables such as permanence of the water body.

In addition, this study is a good example of the application of a multiproxy approach to choose the most realistic paleoclimatic scenario by using different indicators. For instance, petrophysical parameters such as magnetic susceptibility and sediment density could indicate either an increasing runoff, due to higher rainfall, or a low lake level and even desiccation events. Both interpretations are potentially plausible, being difficult to decide which is the correct if there are no other indicators available. In this context, ostracod faunal analysis allows to define the most plausible paleoclimatic scenario for the last 3000 years in Cari-Laufquen area.

## Acknowledgements

The authors thank the Patagonian Lake Drilling Project (PATO/PALATRA) team members and the technical support of P. Troyón with SEM photos.

## Funding

This work was supported by the National Council of Science and Technology Research of Argentina, CONICET under Grant PIP 00819, PIP 0021; the National Agency for the Promotion of Science and Technology under Grant PICT 0082, PICT 2014-1271; and the National University of Comahue under Grant UNCo 04/B166 and 04/B194. DA acknowledges financial support from the Swiss National Science Foundation (projects NF200021-1006668/1, NF200020-111928/1, NF200021-155927/1 and NF200021-155927/2).

## References

- Ariztegui D, Bösch P and Davaud E (2007) Dominant ENSO frequencies during the Little Ice Age in Northern Patagonia: The varved record of proglacial Lago Frías, Argentina. *Quaternary International* 161: 46–55.
- Ariztegui D, Anselmetti FS, Gilli A et al. (2008) Late Pleistocene environmental changes in Patagonia and Tierra del Fuego – A limnogeological approach. In: Rabassa J (ed.) *The Late Cenozoic of Patagonia and Tierra del Fuego (Developments in Quaternary Science, vol. 11)*. London: Elsevier, pp. 241–253.

- Ariztegui D, Anselmetti FS, Seltzer GO et al. (2001) Identifying paleoenvironmental change across South and North America using high-resolution seismic stratigraphy in lakes. In: Markgraf V (ed.) *Interhemispheric Climate Linkages*. San Diego, CA: Academic Press, pp. 227–240.
- Bertrand S, Boës X, Castiaux J et al. (2005) Temporal evolution of sediment supply in Lago Puyehue (Southern Chile) during the last 600 yr and its climatic significance. *Quaternary Research* 64: 163–175.
- Boës X and Fagel N (2007) Relationships between southern Chilean varved lake sediments, precipitation and ENSO for the last 600 years. *Journal of Paleolimnology* 39: 237–252.
- Boomer I, Horne DJ and Slipper IJ (2003) The use of ostracods in palaeoenvironmental studies, or what can you do with an ostracod shell? *The Paleontological Society Papers* 9: 153–179.
- Bradbury JP, Grosjean M, Stine S et al. (2001) Full and late glacial records along the PEP1 transect: Their role in developing interhemispheric paleoclimate interactions. In: Markgraf V (ed.) *Interhemispheric Climate Linkages*. San Diego, CA: Academic Press, pp. 265–292.
- Cartwright A, Quade J, Stine S et al. (2011) Chronostratigraphy and lake-level changes of Laguna Cari-Laufquén, Río Negro, Argentina. *Quaternary Research* 76: 430–440.
- Charlet F, De Batist M, Chapron E et al. (2008) Seismic stratigraphy of Lago Puyehue (Chilean Lake District): New views on its deglacial and Holocene evolution. *Journal of Paleolimnology* 39: 163–177.
- Chávez-Lara CM, Roy PD, Caballero MM et al. (2012) Lacustrine ostracodes from the Chihuahuan Desert of Mexico and inferred Late Quaternary paleoecological conditions. *Revista Mexicana de Ciencias Geológicas* 29: 422–431.
- Clarke KR and Gorley RN (2005) *PRIMER v.6: User Manual / Tutorial*. Plymouth: PRIMER-E Ltd.
- Clarke KR and Warwick RM (2001) *Change in Marine Communities: An Approach to Statistical Analysis and Interpretation*. Plymouth: Plymouth Marine Laboratory.
- Coira GL (1979) Descripción geológica de la Hoja 40D, Ingeniero Jacobacci. *Servicio Geológico Nacional* 168: 1–84.
- Coviaga CA (2016) *Ostrácosos lacustres actuales de Patagonia Norte y su correspondencia con secuencias holocénicas*. PhD Thesis, Universidad Nacional del Comahue.
- Coviaga CA, Cusminsky GC and Pérez AP (2018a) Ecology of freshwater ostracods from Northern Patagonia and their potential application in paleo-environmental reconstructions. *Hydrobiologia* 816(1): 3–20.
- Coviaga CA, Cusminsky GC, Bacalá N et al. (2015) Dynamics of ostracod populations from shallow lakes of Patagonia: Life history insights. *Journal of Natural History* 49: 1023–1045.
- Coviaga CA, Pérez AP, Ramos LY et al. (2018b) On two species of *Riocypis* (Crustacea, Ostracoda) from Northern Patagonia and their relation to *Eucypris fontana*; implications in paleo-environmental reconstructions. *Canadian Journal of Zoology* 96: 801–817.
- Coviaga CA, Rizzo A, Pérez AP et al. (2017) Reconstruction of the hydrologic history of a shallow Patagonian steppe lake during the past 700 yr, using chemical, geologic, and biological proxies. *Quaternary Research* 87: 208–226.
- Curry B, Henne PD, Mezquita-Joanes F et al. (2016) Holocene paleoclimate inferred from salinity histories of adjacent lakes in southwestern Sicily (Italy). *Quaternary Science Reviews* 150: 67–83.
- Cusminsky GC and Whatley RC (1996) Quaternary non-marine ostracods from lake beds in northern Patagonia. *Revista Española de Paleontología* 11: 143–154.
- Cusminsky G, Schwalb A, Pérez AP et al. (2011) Late quaternary environmental changes in Patagonia as inferred from lacustrine fossil and extant ostracods. *Biological Journal of the Linnean Society* 103: 397–408.
- Cusminsky GC, Pérez AP, Schwalb A et al. (2005) Recent Lacustrine Ostracods from Patagonia, Argentina. *Revista Española de Micropaleontología* 37: 431–450.
- D'Ambrosio DS, Diaz AR, Garcia A et al. (2015) First description of the soft part anatomy of *Ilyocypris ramirezi* Cusminsky and Whatley (Crustacea, Ostracoda) from Argentina, South America. *Zootaxa* 3957: 59–68.
- De Deckker P (2002) Ostracod palaeoecology. The Ostracoda: Applications in quaternary research. *Geophysical Monograph* 131: 121–134.
- Departamento Provincial de Aguas. Provincia de Río Negro (2011) *Lagunas Carrilauquen*.
- Diaz M and Pedrozo F (1996) Nutrient limitation in Andean-Patagonian lakes at latitude 40–41°S. *Archiv für Hydrobiologie* 138: 123–143.
- Dubois DM (1973) An index of fluctuations, D0, connected with diversity and stability of ecosystems: Applications in the Lotka-Volterra model and in an experimental distribution of species. Rapport de synthèse III, Programme national sur l'environnement physique et biologique, Projet Mer. Commission Interministérielle de la Politique Scientifique, Liège.
- Elbert J, Wartenburger R, Von Gunten L et al. (2013) Late-Holocene air temperature variability reconstructed from the sediments of Laguna Escondida, Patagonia, Chile (45°30'S). *Palaeogeography, Palaeoclimatology, Palaeoecology* 369: 482–492.
- Fontana S and Ballent S (2005) A new giant cypridid ostracod (Crustacea) from southern Buenos Aires Province, Argentina. *Hydrobiologia* 533: 187–197.
- Forester RM (1988) *Nonmarine Calcareous Microfossil Sample Preparation and Data Acquisition Procedures*. U.S. Geological Survey Technical Procedure HP-78 RI, pp. 1–9.
- Galloway RW, Markgraf V and Bradbury JP (1988) Dating shorelines of lakes in Patagonia, Argentina. *Journal of South American Earth Sciences* 1: 195–198.
- Garreaud R, Vuille M, Compagnucci R et al. (2009) Present-day South American Climate. PALAEO3 Special issue (LOTRED South America). *Palaeogeography, Palaeoclimatology, Palaeoecology* 281: 180–195.
- Gilli A, Ariztegui D, Anselmetti F et al. (2005) Mid-Holocene strengthening of the Southern Westerlies in South America – Sedimentological evidences from Lago Cardiel, Argentina (49°S). *Global and Planetary Change* 49: 75–93.
- Glasser NF, Harrison S, Winchester V et al. (2004) Late Pleistocene and Holocene palaeoclimate and glacier fluctuations in Patagonia. *Global and Planetary Change* 43: 79–101.
- Grimm E (1987) CONISS: A Fortran 77 program for stratigraphically constrained cluster analysis by the method of incremental sum of squares. *Computational Geosciences* 13: 13–35.
- Grimm E (1991) *Tilia and Tilia Graph. Research and Collection Center*. Springfield, IL: Illinois State Museum.
- Guerra L, Piovano EL, Córdoba FE et al. (2015) The hydrological and environmental evolution of shallow Lake Melincué, central Argentinean Pampas, during the last millennium. *Journal of Hydrology* 529: 570–583.
- Guilizzoni P, Massafiero J, Lami A et al. (2009) Palaeolimnology of Lake Hess (Patagonia, Argentina): Multi-proxy analyses of short sediment cores. *Hydrobiologia* 631: 289–302.
- Hogg AG, Hua Q, Blackwell PG et al. (2013) SHCal13 Southern Hemisphere Calibration, 0–50,000 Years cal BP. *Radiocarbon* 55(2): 1–15.
- Holmes JA (2001) Ostracoda. In: Smol SP, Birks HJB and Last WM (eds) *Tracking Environmental Change Using Lake Sediments*. Dordrecht: Kluwer Academic Publishers, pp. 125–151.
- Holmes JA, Fothergill PA, Street-Perrott FA et al. (1998) A high-resolution Holocene ostracod record from the Sahel zone

- of Northeastern Nigeria. *Journal of Paleolimnology* 20: 369–380.
- Horne DJ, Cohen A and Martens K (2002) Taxonomy, morphology and biology of quaternary and living Ostracoda. In: Holmes JA and Chivas A (eds) *The Ostracoda: Applications in Quaternary Research*. Washington, DC: American Geophysical Union, pp. 6–36.
- Iglesias V, Whitlock C, Bianchi MM et al. (2011) Holocene climate variability and environmental history at the Patagonian forest/steppe ecotone: Lago Mosquito (42°29'37.89"S, 71°24'14.57"W) and Laguna del Condor (42°20'47.22"S, 71°17'07.62"W). *The Holocene* 22: 1297–1307.
- Irurzun MA, Gogorza CSG, Sinito AM et al. (2014) A high-resolution palaeoclimate record for the last 4800 years from lake la Brava, SE pampas plains, Argentina. *Geofísica Internacional* 53: 365–383.
- Jenny B, Valero-Garcés BL, Urrutia R et al. (2002) Moisture changes and fluctuations of the Westerlies in Mediterranean Central Chile during the last 2000 years: The Laguna Aculeo record. *Quaternary International* 87: 3–18.
- Juggins S (2003) *C2 User Guide. Software for Ecological and Palaeoecological Data Analysis and Visualization*. Newcastle upon Tyne: University of Newcastle.
- Karanovic I (2012) *Recent Freshwater Ostracods of the World: Crustacea, Ostracoda, Podocopida*. Heidelberg: Springer.
- Keatings K, Holmes J, Flower R et al. (2010) Ostracods and the Holocene palaeolimnology of Lake Qarun, with special reference to past human–environment interactions in the Faiyum (Egypt). *Hydrobiologia* 654: 155–176.
- Keatings KI, Hawkes W, Holmes JA et al. (2007) Evaluation of ostracod-based palaeoenvironmental reconstruction with instrumental data from the arid Faiyum Depression, Egypt. *Journal of Palaeolimnology* 38: 261–283.
- Laprida C, Massafiero J, Ramon Mercau J et al. (2014) Paleobio-indicadores del fin del mundo: Ostrácodos y quironómidos del extremo sur de Sudamérica en ambientes lacustres cuaternarios. *Latin American Journal of Sedimentology and Basin Analysis* 21(2): 97–117.
- Lara A and Villalba R (1993) A 3620-year temperature record from Fitzroya cupressoides tree rings in southern South America. *Science* 260: 1104–1106.
- Li X and Liu W (2014) Water salinity and productivity recorded by ostracod assemblages and their carbon isotopes since the early Holocene at Lake Qinghai on the northeastern Qinghai-Tibet Plateau, China. *Palaeogeography, Palaeoclimatology, Palaeoecology* 407: 25–33.
- Luckman BH and Villalba R (2001) Assessing the synchronicity of glacier fluctuations in the western Cordillera of the Americas during the last millennium. In: Markgraf V (ed.) *Interhemispheric Climate Linkages*. San Diego, CA: Academic Press, pp. 119–140.
- Mancini MV (2001) Pollen analysis of a high Andean site during the Late-Holocene: Cerro Verlika 1, southwest Santa Cruz, Argentina. *Ameghiniana* 38: 455–462.
- Marco-Barba J, Mesquita-Joanes F and Miracle M (2013a) Ostracod palaeolimnological analysis reveals drastic historical changes in salinity, eutrophication and biodiversity loss in a coastal Mediterranean lake. *The Holocene* 23: 556–567.
- Marco-Barba J, Holmes JA, Mesquita-Joanes F et al. (2013b) The influence of climate and sea-level change on the Holocene evolution of a Mediterranean coastal lagoon: Evidence from ostracod palaeoecology and geochemistry. *Geobios* 46: 409–421.
- Margalef R (1974) *Ecología*. Barcelona: Ed. Omega.
- Markgraf V (1983) Late and postglacial vegetational and paleoclimatic changes in sub-Antarctic, temperate and arid environments in Argentina. *Palynology* 7: 43–70.
- Markgraf V, Bradbury JP, Schwalb A et al. (2003) Holocene palaeoclimates of southern Patagonia: Limnological and environmental history of Lago Cardiel, Argentina. *The Holocene* 13: 581–591.
- Meisch C (2000) *Freshwater Ostracoda of Western and Central Europe* (Süsswasserfauna von Mitteleuropa 8/3). Heidelberg: Spektrum Akademischer Verlag.
- Mercer JH (1970) Variations of some Patagonian glaciers since the Late-Glacial: II. *American Journal of Science* 269: 1–25.
- Meyers PA and Lallier-Vergès E (1999) Lacustrine sedimentary organic matter records of Late Quaternary paleoclimates. *Journal of Paleolimnology* 21: 345–372.
- Mezquita F, Roca JR, Reed JM et al. (2005) Quantifying species–environment relationships in non-marine Ostracoda for ecological and palaeoecological studies: Examples using Iberian data. *Palaeogeography, Palaeoclimatology, Palaeoecology* 225: 93–117.
- Mischke S, Herzsich U, Zhang C et al. (2005) A Late Quaternary lake record from the Qilian Mountains (NW China): Lake level and salinity changes inferred from sediment properties and ostracod assemblages. *Global and Planetary Change* 46: 337–359.
- Mischke S, Kramer M, Zhang C et al. (2008) Reduced early Holocene moisture availability in the Bayan Har Mountains, northeastern Tibetan Plateau, inferred from a multi-proxy lake record. *Palaeogeography, Palaeoclimatology, Palaeoecology* 267: 59–76.
- Moy C, Moreno P, Dunbar R et al. (2009) Climate change in Southern South America during the last two millennia. In: Vimeux F, Sylvestre F and Khodri M (eds) *Climate Change in Southern South America during the Last Two Millennia: Developments in Paleoenvironmental Research 14*. New York: Springer, pp. 353–393.
- Ohlendorf C, Fey M, Massafiero J et al. (2014) Late-Holocene hydrology inferred from lacustrine sediments of Laguna Chálitel (southeastern Argentina). *Palaeogeography, Palaeoclimatology, Palaeoecology* 411: 229–248.
- Pacton M, Hunger G, Martinuzzi V et al. (2015) Organomineralization processes in freshwater stromatolites: A living example from eastern Patagonia. *The Depositional Record* 1(2): 130–146.
- Peng P, Zhu L, Frenzel P et al. (2013) Water depth related ostracod distribution in Lake Pumoyum Co, southern Tibetan Plateau. *Quaternary International* 313–314: 47–55.
- Pineda D (2008) *Estudio Micropaleontológico (Clase Ostracoda) en un perfil Cuaternario del Área de Cari-Laufquen, Patagonia, Argentina: Inferencias paleoambientales*. Degree Thesis, Universidad Nacional del Comahue.
- Piovano EL, Ariztegui D and Moreira SD (2002) Recent environmental changes in Laguna Mar Chiquita (central Argentina): A sedimentary model for a highly variable saline lake. *Sedimentology* 49: 1371–1384.
- Ramón-Mercau J and Laprida C (2016) An ostracod-based calibration function for electrical conductivity reconstruction in lacustrine environments in Patagonia, Southern South America. *Ecological Indicators* 69: 522–532.
- Ramón-Mercau J, Laprida C, Massafiero J et al. (2012) Patagonian ostracods as indicators of climate related hydrological variables: Implications for paleoenvironmental reconstructions in Southern South America. *Hydrobiologia* 694: 235–251.
- Ramos L, Cusminsky G, Schwalb A et al. (2017) Morphotypes of the lacustrine ostracod *Limnocythere rionegroensis* Cusminsky and Whatley from Patagonia, Argentina, shaped by aquatic environments. *Hydrobiologia* 786: 137–148.
- Recasens C, Ariztegui D, Gebhardt C et al. (2011) New insights into paleoenvironmental changes in Laguna Potrok Aike,



- southern Patagonia, since the Late Pleistocene: The PASADO multiproxy record. *The Holocene* 22: 1323–1335.
- Reissig M, Trochine C, Queimaliños C et al. (2006) Impact of fish introduction on planktonic food webs in lakes of the Patagonian Plateau. *Biological Conservation* 132: 437–447.
- Schäfer HW (1943) Über zwei neue deutsche Arten der Süßwasser-Ostracoden. *Zoologischer Anzeiger* 143(9/10): 210–216.
- Schwalb AJ, Burns S, Cusminsky G et al. (2002) Assemblage diversity and isotopic signals of modern ostracodes and host waters from Patagonia, Argentina. *Palaeogeography, Palaeoclimatology, Palaeoecology* 187: 323–339.
- Sepúlveda J, Pantoja S, Hughen KA et al. (2009) Late-Holocene sea-surface temperature and precipitation variability in northern Patagonia, Chile (Jacaf Fjord, 44°S). *Quaternary Research* 72: 400–409.
- Shannon CE and Weaver W (1963) *The Mathematical Theory of Communication*. Urbana, IL: University of Illinois Press.
- ter Braak CJF (1987) CANOCO - a Fortran program for canonical community ordination by [partial] [detrended] [canonical] correspondence analysis, principal component analysis and redundancy analysis (version 2.1). Wageningen: Agricultural Mathematics Group, 95 pp.
- ter Braak CJF and Prentice IC (1988) A theory of gradient analysis. *Advances in Ecological Research* 18: 271–317.
- Vargas-Ramirez L, Roche E, Gerrienne P et al. (2008) A pollen-based record of late glacial-Holocene climatic variability in the southern lake district, Chile. *Journal of Paleolimnology* 2: 197–217.
- Vavra W (1898) Süßwasser-Ostracoden. *Ergebn. Hamburger Magalh. Sammelreise 1892–1893. Naturhist Mus Hamburg* 2: 1–26.
- Villalba R (1994) Tree-ring and glacial evidence for the Medieval Warm Epoch and the Little Ice Age in Southern South America. *Climatic Change* 26: 183–197.
- Whatley RC and Cusminsky GC (1999) Lacustrine Ostracoda and late Quaternary palaeoenvironments from the Lake Cari-Laufquen region, Rio Negro province, Argentina. *Palaeogeography, Palaeoclimatology, Palaeoecology* 151: 229–239.
- Zhu J, Lücke A, Wissel H et al. (2013) The last Glacial–Interglacial transition in Patagonia, Argentina: The stable isotope record of bulk sedimentary organic matter from Laguna Potrok Aike. *Quaternary Science Reviews* 71: 205–218.